Supplemental Figures

A

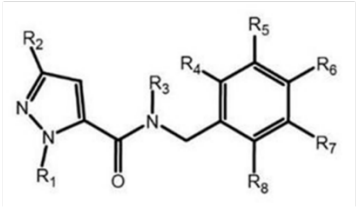

B

compound	R_1	R_2	R_3	R_4	R_5	R_6	R_7	R_8	EC_{50}(μM)
PAV-770	Me	t-Bu	H	O-CH_2-	CH_2-O-	H	F	H	1 - 3
PAV-868	Me	t-Bu	H	OMe	OMe	OMe	H	H	> 3
PAV-858	Me	t-Bu	H	OMe	H	OMe	OMe	H	> 3
PAV-772	Me	t-Bu	H	OMe	F	H	F	H	3
PAV-736	CH_2CH_2OH	t-Bu	H	OMe	OMe	H	H	H	> 3
PAV-869	Me	t-Bu	H	OPr	OMe	H	H	H	> 3
PAV-773	Me	t-Bu	H	OMe	OMe	H	H	H	< 1
PAV-1866	Me	t-Bu	Me	OMe	OMe	H	H	H	> 3
PAV-834	Me	Me	H	OMe	OMe	H	H	H	3
PAV-854	Me	Cy-hex	H	OMe	OMe	H	H	H	> 1
PAV-530	Me	iPr	H	OMe	OMe	H	H	H	1
PAV-835	Me	cyPr	H	OMe	OMe	H	H	H	< 1
PAV-895	Me	cyPr	H	OMe	Me	H	H	H	2
PAV-039	Me	cyPr	H	OMe	OMe	H	H	F	1
PAV-896	Me	cyPr	H	Me	OMe	H	H	H	1.5
PAV-700	Me	cyPr	H	Cl	OMe	H	H	H	2
PAV-235	Me	cyPr	H	F	OMe	H	H	H	0.2
PAV-944	Me	cyPr	H	OMe	CF_3	H	H	H	0.2
PAV-901	Me	cyPr	H	CF_3	OMe	H	H	H	0.3
PAV-671	Me	cyPr	H	H	Cl	OCF_3	H	H	0.05
PAV-774	Me	cyPr	H	Cl	OCF_3	H	H	H	0.2
PAV-431	Me	cyPr	H	OMe	OCF_3	H	H	H	< 0.1
PAV-528	Me	cyPr	H	$OCHF_2$	$OCHF_2$	H	H	H	< 0.1
PAV-877	Me	cyPr	H	H	Me	$OCHF_2$	Me	H	> 2

Supplemental Figure 1. **Early SAR exploration within hit chemical series. Supplemental Figure 1A** shows a Markush structure for the initial hit chemical series in the CFPSA flu capsid assembly screen. **Supplemental Figure 1B** shows the initial structure-activity-relationship pursued to characterize how changes to different parts of the molecule affect activity of the series. EC50 for each compound was determined by $TCID_{50}$ with infectious FLUV in MDCK cells.

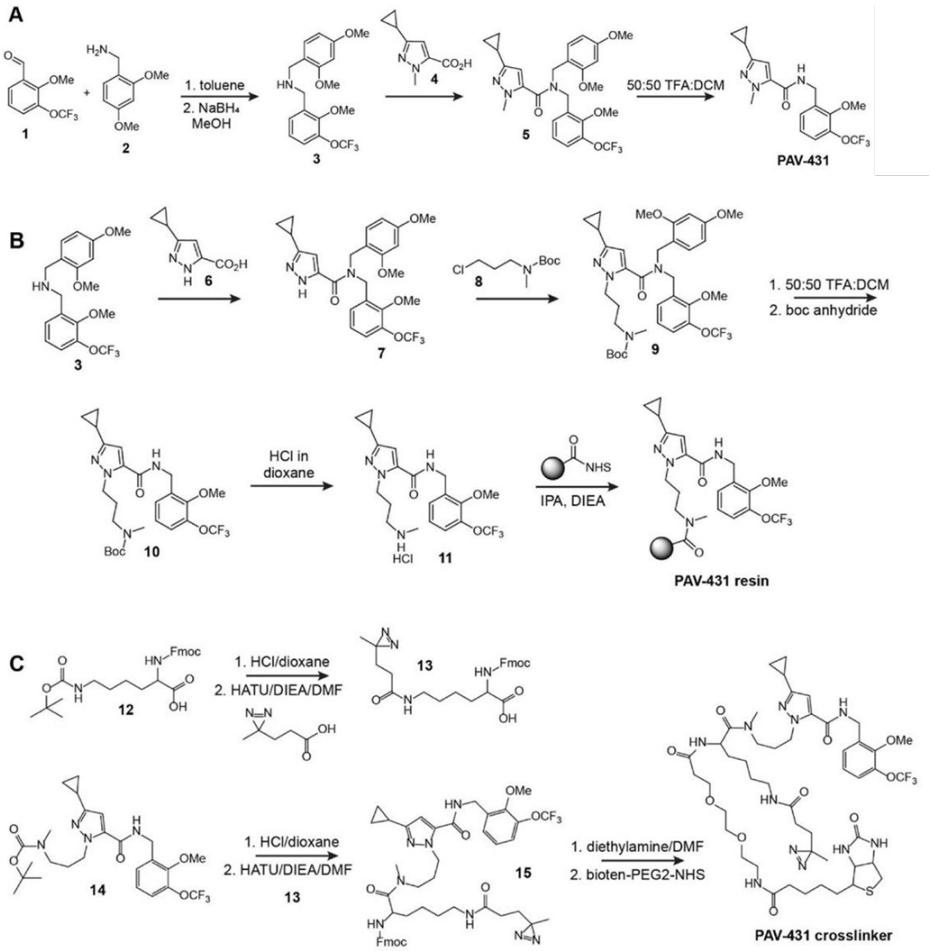

Supplemental Figure 2. Synthetic scheme for PAV-431 and its resin and photocrosslinker analogs. **Supplemental Figure 2A** shows the synthetic scheme for PAV-431. **Supplemental Figure 2B** shows the synthetic scheme for attachment to a resin by the pyrazole position, which was used in the eDRAC experiments described in Figure 5 and Supplemental Figure 4. The eDRAC experiments described in Figure 6 were conducted with a resin attached from the benzyl ring. **Supplemental Figure 2C** shows the synthetic scheme for the PAV-431 photocrosslinker analog used in the experiments described in Figure 6.

A

Compounds Parameters		PAV-431		
EC_{90} (nM)		100		
MW		369.3		
Mouse MTD	Route- Dosage, mg/kg Safe dose	-	IP-5	-
Rat PK	Route- Dosage, mg/kg	IV-1	IP-5	PO-5
	AUC_{last}, h.ng/mL	307	910	Low conc.
	AUC_{inf}, h.ng/mL	342	923	
	C_{max}, ng/mL	253	293	
	T_{max}, h	0.08	0.25	
	$t_{1/2}$, h	12	5	
	CL, mL/min	49	-	
	V_{z}, L/Kg	32	-	
	F, %	-	59	
Rat Uptake	Route- Dosage, mg/kg	-	IP-5	-
	Conc. In Lungs, ng/g, 0.5h, 2h	-	452, 131	-
	Conc. in Brain, ng/g, 0.5h, 2h	-	593, 177	-
	Conc. in Plasma, ng/mL, 0.5h, 2h	-	308, 123	-

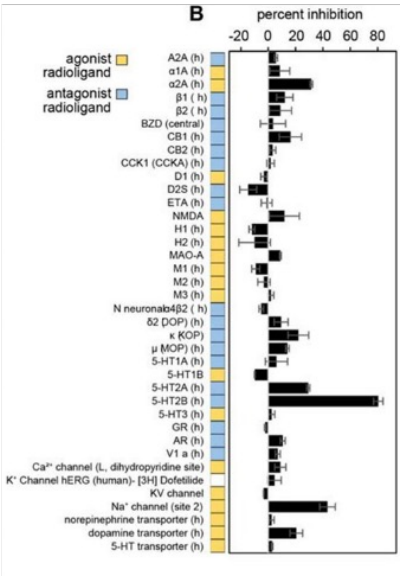

Supplemental Figure 3. **Supplemental Figure 3A** shows the drug-like properties of PAV-431 including in vivo and in vitro assessments of toxicity as well as pharmacokinetic properties. Maximum tolerated dose (MTD) studies in mice were conducted using female Balb/c mice where randomized groups containing 3 mice were dosed with a single dose of vehicle or compound and monitored for 48 hours for symptoms of toxicity. Pharmacokinetic (PK) studies were conducted in male Sprague Dawley rats where randomixed groups of four animals were administered compound and plasma was collected before dosing then after 5 minutes, 15 minutes, 30 minutes, 1 hour, 2 hours, 4 hours, 8 hours, 12 hours, and 24 hours to determine concentration of the compound in plasma over time. In the uptake studies, animals were euthanized after 30 minutes or 2 hours to determine concentration of the compound in the lung and brain. **Supplemental Figure 3B** shows the results of PAV-431 in an in vitro Cerep panel, a commercial screen for potential to bind to a broad panel of receptors, enzymes, and ion channels, reported as percent inhibition of control specific binding. PAV-431 was tested at 50uM, a concentration ~500x higher than antiviral EC50. Data shown are the averages of replicates, error bars indicate standard error.